Parametric Modeling and Estimation of Acoustic Sediment Properties Using a System Identification Approach

Zobeida Cisneros, Luc Peirlinckx, and Leo Pierre Van Biesen

Abstract— **The acoustic properties of marine sediments are measured to obtain an acoustic signature of their mechanical characteristics. The proposed 1-D wave propagation model accounts for absorption and dispersion. Use is made of an inverse procedure based on a maximum likelihood estimator for obtaining a parametric identification of the sediments. Measurements are performed in the laboratory, in reflection and transmission modes, on prepared samples of natural sediments, at normal incidence, and using a controlled measurement environment in the frequency range of 300 to 700 kHz. The model validation is performed for a water layer, an ideal medium with little absorption and dispersion, and for a silty-clay layer. A comparison between the estimated and measured amplitude and phase characteristics for these two media indicates that the parametric identification of the silty-clay is successful. For both media, comparable differences, of 0.3 dB maximum for the amplitude and three degrees for the phase, are observed.**

I. Introduction

THOUGH THE study of marine sediments and their functional relation with acoustic properties has been carried out since the 1950's [1]–[6], it is not yet possible to fully accomplish the identification of the sediment's characteristics through remote acoustic measurements, especially for those frequently changing facies in an estuarine site. We will focus on this problem using a system identification approach and proposing a model that considers the losses due to absorption and dispersion along the propagation of the wave through the sediment. This is carried out by means of a rational form model, which proved successful for describing absorption and dispersion on quasi-linear homogeneous isotropic viscoelastic composites [7]. Although marine sediments do not fully fulfil the same constraints as the composites, it is known that their mechanical behavior falls within the domain of viscous, elastic, or a combination of both responses to applied stresses of various characteristics. Moreover, Bjørnø [8] shows that the high absorption at sand-silt saturated sediments when using a high-intensity sound source masks out the nonlinearity expected for these assemblages.

We study the nonconsolidated sediments that constitute the top most layers of the marine sedimentary record (1 m of bottom depth). Briefly stated, marine sediments can be differentiated on the basis of their main grain size component(s), e.g., medium sands or silty sands, well or poorly sorted sands. But their mechanical response, not always explained by this sole characteristic, strongly depends on the geodynamic setup of the site. Sediments may be deposited after a short residence time in the water column, or reworked and resettled, and consequently their rigidity, porosity, and permeability are accordingly established. They may have also undergone a release of overburden hydrostatic pressure by the new equilibrium set following an erosion event. Interestingly, they may or may not belong to the actual environment, since sea transgressions and regressions accompanied by deposition and erosion are the building agents of the recent upper sedimentary layers. Generally, fine grained sediments (muds) are expected to have high viscosity and plasticity and to act as a homogenous and isotropic medium. Nevertheless, particular mechanical properties may be caused by the presence of flocks and aggregates. The latter are frequently present in estuarine environments and may be preserved even at depths of several meters (see [9] and [10]). Sands, on the other hand, have no cohesion and are highly permeable, especially if they are coarse and well sorted. To show acoustically that the difference is marked, data of the work by Saclantcen [11] are used to build Fig. 1, where the distinct relations of impedance—calculated as $\rho \times Vp$—versus density at muds and sands is depicted. Density (ρ) and the compressional velocity Vp (Vp measured at 400 kHz) are parameters measured on cores of the Adriatic Sea, with Vp corrected for field conditions. The correlation coefficients $R^2 = 96\%$ and 99% for two muds deposited in different environments indicate that the density reveals a good marker of the acoustic response and supports the assumption that they can be modeled as a homogeneous, one-phase element. Stoll, Hampton [4], [5], [12], and others have observed this same behavior over a wider range of frequencies. The less satisfactory correlation observed for the sand data, nevertheless, indicates that the bulk density solely does not control the acoustic response and suggests that the assumption of isotropy and homogeneity of a one-phase medium used for our modeling may not be realistic.

The example in Fig. 1 shows a slightly different trend of impedance for each of the mud samples. If high accuracy is needed, e.g., to differentiate the hemipelagic and the Holocene mud of the Adriatic Sea, it is important that a particular set of data is gathered for one and the other environment. Generalizing the results to any other silty-clay that may have undergone different history of deposition, or may have changed its internal structure due to chemical or biological agents would be of small use. Certain laboratory procedures

Manuscript received November 4, 1994; revised May 26, 1995.

The authors are with the Department of Fundamental Electricity and Instrumentation (ELEC), Vrije Universiteit Brussel, B-1050, Brussels, Belgium.

IEEE Log Number 9415000.

0885–3010/95$04.00 © 1995 IEEE

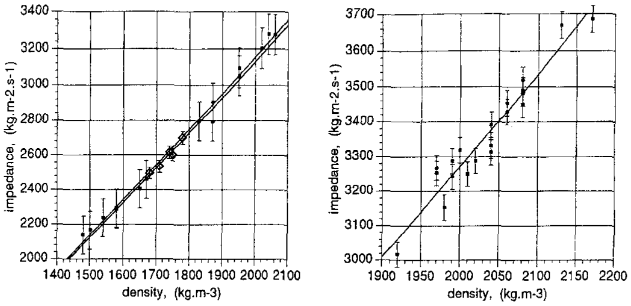

(a) (b)

Fig. 1. Comparison of the impedance as a function of density for mud (a) and sand (b). Graphs show the standard error of the impedance: (a) hemipelagic mud (◇) and Holocene mud (■) and (b) along shore and relict sands (■).

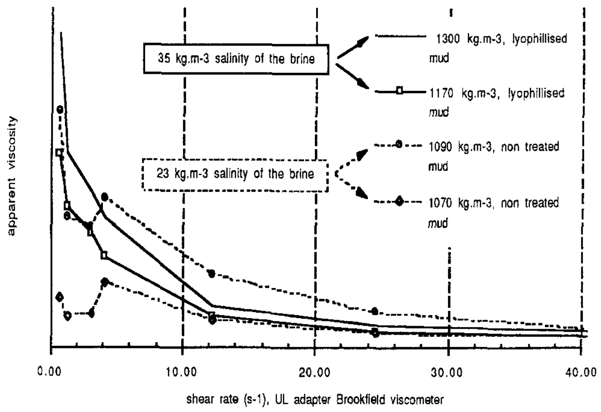

Fig. 2. Different trends of viscosity for treated and nontreated samples. Geology Department, Lafayette College, Easton, PA, USA.

may also affect a sample's response, as, for instance, removal of the organic matter or lyophillization to bring the sample to a fully dried powder. Fig. 2 presents the dynamic response to a shearing stress. The continuous line corresponds to a silty-clay free of organic matter brought back to a slurry after being lyophillized. Shear thickening, well known for muds that preserve their original structure [13], [14], is absent, whereas it can be observed between 2 and 10 Hz for the nontreated mud represented by the dashed line.

For our work, a silty-clay (mud) sample and a sand sample were tested. The silty-clay belongs to the Boom Clay (type locality in Boom, Belgium), an originally marine deposited mud that presently lays in continental environment (great part of it) after regressions of the sea. It was brought to a density of 1330 kg $\cdot$ m^{-3} by dilution with demineralized water, had not been lyophillized, and held its original content of organic matter. Its granulometric distribution is shown in Fig. 3, where Φ stands for the $-\log_2$ (diameter of the grains in millimeters). The second sample is sand made of quartz mainly, of very fine to medium size particles in the range of (74, 351) μm in Tyler sieve scale. Its organic matter had been removed and it was saturated with demineralized water up to a density of 2040 kg $\cdot$ m^3.

Next, the identification approach utilized and the discussion over the estimated parameters will be presented, and finally, further improvements will be recommended.

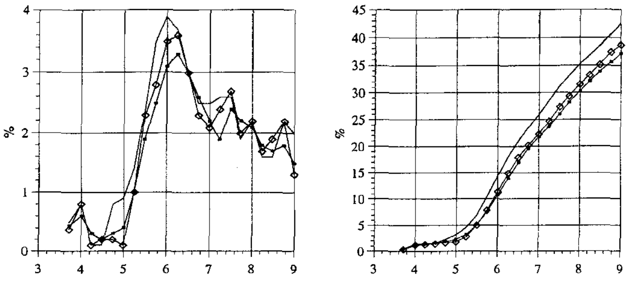

(a) (b)

Fig. 3. Grain size distribution of three subsamples of Boom Clay, Royal Belgian Institute of Natural Sciences, Brussels, Belgium: (a) histogram and (b) frequency cumulative curve.

II. The Modeling Approach and the Experimental Setup

In this section, the modeling of the ultrasonic wave propagation is discussed for a plane parallel multilayer. The ultrasonic wave propagation in the multilayer is described by means of a plane wave theory that incorporates the effects of absorption and dispersion along the layers. Modeling the absorption $\alpha_i(\omega)$ and dispersion $c_i(\omega)$ for the layer (i) is carried out by a rational form that has proven valid and advantageous for visco-elastic composites [7], [15]. The complex wave number $K_i(\omega)$ is defined as follows:

$$K_i(\omega) = \frac{\omega}{V_i(\omega)} = \frac{\omega}{c_i(\omega)} - j \cdot \alpha_i(\omega) \tag{1}$$

with the complex velocity

$$V_i(\omega) = c_{0i}\sqrt{\frac{1+\sum_{l=1}^{N_i}\alpha_{Li,l}(j\omega)^l}{1+\sum_{l=1}^{D_i}\beta_{Li,l}(j\omega)^l}} = c_{0i} \cdot P_i(\omega, \alpha_{Li}, \beta_{Li}). \tag{2}$$

The column vectors α_{Li} and β_{Li} contain the numerator and denominator coefficients of the rational form related to layer (i)

$$\alpha_{Li} = [\alpha_{Li,1}, \cdots, \alpha_{Li,N_i}]^t \text{ and } \beta_{Li} = [\beta_{Li,1}, \cdots, \beta_{Li,D_i}]^t \tag{3}$$

with order N_i and D_i, respectively. c_{0i} represents the frequency independent phase velocity and $P_i(\omega, \alpha_{Li}, \beta_L)$ the function that describes the frequency dependence of the complex velocity at layer (i). The interface reflection and transmission coefficients at the interface between the layers (i) and $(i+1)$ are defined by

$$r_i(\omega) = \frac{P_i(\omega, \alpha_{Li}, \beta_{Li}) - Z_{i,i+1}P_{i+1}(\omega, \alpha_{Li+1}, \beta_{Li+1})}{P_i(\omega, \alpha_{Li}, \beta_{Li}) + Z_{i,i+1}P_{i+1}(\omega, \alpha_{Li+1}, \beta_{Li+1})} \tag{4}$$

and

$$t_i(\omega) = 1 + r_i(\omega). \tag{5}$$

The parameter $Z_{i,i+1}$ is defined as the ratio of the real acoustic impedances Z_i and Z_{i+1} of layers (i) and $(i+1)$

$$Z_{i,i+1} = \frac{Z_i}{Z_{i+1}} = \frac{\rho_i \cdot c_{0i}}{\rho_{i+1} \cdot c_{0i+1}}. \tag{6}$$

Note that this is a real parameter, since only the frequency independent phase velocities as well as the densities ρ_i and

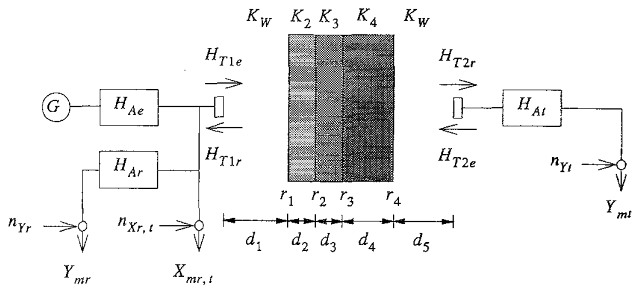

Fig. 4. The measurement setup for the reflection experiment (monostatic mode) and the transmission experiment (bistatic mode).

ρ_{i+1} are introduced for the layers (i) and $(i+1)$. The frequency dependence of the complex acoustic impedance is described by the function $P_i(\omega, \alpha_{Li}, \beta_{Li})$, as defined in (2).

The constituents of the measurement setup for the reflection and transmission experiments are shown in Fig. 4, together with their transfer functions for a multilayer of which layers 1 and 5 are water. The experiments are performed with a pulser–receiver (Panametrics 5055PR) and without repositioning of the sediment samples under investigation. The acquisition of the reflection and transmission experiments is carried out in the monostatic and bistatic mode, respectively. The position of the broadband transducers (center frequency of 500 kHz) is not altered when switching from the monostatic to the bistatic measurement mode.

The characteristics of the emitter $H_{Ae}(\omega)$, the emitting and receiving transducers $H_{Tie}(\omega)$ and $H_{Tir}(\omega)$, respectively, with $i = 1, 2$, as well as the receiving amplifier characteristics for the reflection and transmission experiments $H_{Ar}(\omega)$ and $H_{At}(\omega)$, respectively, are described in the frequency domain. The generated pulses $X_{mr}(\omega)$ and $X_{mt}(\omega)$ (inputs) as well as the reflected signal $Y_{mr}(\omega)$ and transmitted signal $Y_{mt}(\omega)$ (outputs) are digitized. The input and output measurement errors are represented by the random variables n_{X_i} and n_{Y_i}, which have a frequency dependent variance $\sigma^2_{X_i}(\omega)$ and $\sigma^2_{Y_i}(\omega)$, respectively, with $(i = r, t)$.

A calibration experiment is used in order to eliminate the influence of the system setup in the estimation, one for transmission and reflection, respectively. This experiment is performed maintaining the same experimental configuration and close conditions (temperature, water quality, etc.) as the ones present during the test on the sediments.

The transfer function describing the calibration in transmission (bistatic mode) takes the form $H_{\text{calt}}(\omega) = H_{\text{syst}}(\omega) \cdot H_{t0}(\omega)$, where $H_{t0}(\omega)$ represents the wave propagation along the water path (transducer1e/water/transducer2r) and $H_{\text{syst}}(\omega)$ describes the response of the measurement setup. Similarly, the transmission experiment on the sample can be modeled by means of the transfer function $H_{mt}(\omega) = H_{\text{syst}}(\omega) \cdot H_t(\omega)$, where $H_t(\omega)$ describes the wave propagation in the multilayer.

For measurements in reflection, calibration is not possible using the propagation along the water path since transducer 1 acts both as emitter and receiver. An alternative is to measure a plate of Plexiglas placed at a distance d_w from the emitter (optimally $d_w = d_1$). This choice is made by considering the particular measurement setup of our experiments, in which d_2 and d_4 are the widths of the walls of a container built in Plexiglas that holds the sediments in place. By doing so, $H_{\text{syst}}(\omega)$ is obtained from the calibration experiment, and similar transfer functions can be generated for the reflection experiments as the ones describing the transmission case, but the characteristics of the Plexiglas need to be estimated from an extra transmission experiment.

The nonparametric estimates $H^{np}_{mt}(\omega)$ and $H^{np}_{mt}(\omega)$ of the transfer functions $H_{mt}(\omega)$ and $H_{mr}(\omega)$ are obtained from input-output measurements ($X_{mr,t}(\omega)$ and $Y_{mr,t}(\omega)$, see Fig. 4). Combining the nonparametric estimates of the calibration experiments $H^{np}_{\text{calt}}(\omega)$ and $H^{np}_{\text{calr}}(\omega)$ with $H^{np}_{mt}(\omega)$ and $H^{np}_{mr}(\omega)$, the calibrated transmission and reflection coefficients $\tilde{H}_t(\omega, \mathbf{P_t})$ and $\tilde{H}_t(\omega, \mathbf{P_r})$ of the multilayer become available

$$H^{np}_{mt}(\omega) = \tilde{H}_t(\omega, \mathbf{P_t}) \cdot H^{np}_{\text{calt}}(\omega) \tag{7}$$

$$H^{np}_{mr}(\omega) = \tilde{H}_r(\omega, \mathbf{P_r}) \cdot H^{np}_{\text{calr}}(\omega). \tag{8}$$

The separation into numerators and denominators, as required for the estimator, is carried out as follows:

$$\tilde{H}_r(\omega, \mathbf{P_r}) = \frac{N_r(\omega, \mathbf{P_r})}{D(\omega, \mathbf{P_c})} \quad \text{and} \quad \tilde{H}_t(\omega, \mathbf{P_t}) = \frac{N_t(\omega, \mathbf{P_t})}{D(\omega, \mathbf{P_c})} \tag{9}$$

with

$$N_r(\omega, \mathbf{P_r}) = e^{-j\omega\tau_r}\{(r_1 + r_2 e^{-2jK_2d_2})(1 + r_3r_4e^{-2jK_4d_4}) + (r_1r_2 + e^{-2jK_2d_2})(r_3 + r_4e^{-2jK_4d_4})e^{-2jK_3d_3}\} \tag{10}$$

and

$$N_t(\omega, \mathbf{P_t}) = t_1t_2t_3t_4e^{j\omega\tau_t} \cdot e^{-jK_2d_2} \cdot e^{-K_3d_3} \cdot e^{-jK_4d_4}. \tag{11}$$

The common denominator is given by

$$D(\omega, \mathbf{P_c}) = (1 + r_1r_2e^{-2jK_2d_2})(1 + r_3r_4e^{-2jK_4d_4}) + (r_2 + r_ie^{-2jK_2d_2})(r_3 + r_4e^{-2jK_4d_4})e^{-2jK_3d_3}. \tag{12}$$

The numerators $N_r(\omega, \mathbf{P_r})$ and $N_t(\omega, \mathbf{P_t})$ depend on the vectors $\mathbf{P_r} = \{\tau_r, \mathbf{P_c}\}$ and $\mathbf{P_t} = \{\tau_t, \mathbf{P_c}\}$, which contain the model parameters including the external delays τ_r and τ_t. The delay τ_r introduced for the calibrated reflection coefficient will differ from zero when the calibration experiment is carried out at a distance d_W different from d_1. On the other hand, for the transmission experiments, τ_t is always

$$\tau_t = \frac{d_2 + d_3 + d_4}{c_{0W}} \tag{13}$$

where c_{0W} is the dispersionless phase velocity in water. The absorption and dispersion in water are neglected in the considered frequency range of 300 to 700 kHz. The arguments of the exponentials appearing in (10)–(12) are then given by

$$K_id_i = \frac{\omega}{c_{0i}P_i(\omega, \alpha_{Li}, \beta_{Li})}d_i = \frac{\omega\tau_i}{P_i(\omega, \alpha_{Li}, \beta_{Li})} \quad \text{with} \quad i = 2, 3, 4. \tag{14}$$

Finally, the vector $\mathbf{P_c}$ contains the set of common model parameters by introducing the vector $\mathbf{P_{Li}}$ for each layer

$$\mathbf{P_c} = \{\mathbf{P_{L2}}, \mathbf{P_{L3}}, \mathbf{P_{L4}}\} \quad \text{with} \quad \mathbf{P_{Li}} = \{\tau_i, Z_{i,i+1}, \alpha_{Li}, \beta_{Li}\}. \tag{15}$$

Note that since layer 1 is identical to layer $n+1=5$ (water), the following relation exists between the parameters $Z_{i,i+1} (i = 1, \cdots, n)$:

$$\prod_{i=1}^{n} Z_{i,i+1} = 1 \quad \text{with} \quad n = 4 \tag{16}$$

which implies that only $n-1=3$ of them can be estimated. However, assuming that the acoustic impedance of water is known *a priori*, the acoustic impedances $Z_i = \rho_i c_{0i}$ of the other layers can be derived from the estimated parameters $Z_{i,i+1}$.

In our particular case, reflection and transmission experiments are treated using a symmetrical Plexiglas structure (container) constructed with identical Plexiglas plates ($d_2 = d_4 = 0.01$ m, see Fig. 4). The thickness d_3 of the third (sediment) layer equals 0.02 m. Due to the symmetry, the complex wave numbers are given by

$$K_3 = K_{\text{sample}} \quad K_2 = K_4 = K_{\text{plexi}} \tag{17}$$

resulting in the following relations between the interface reflection coefficients:

$$r_3 = -r_2 \quad r_4 = -r_1. \tag{18}$$

This reduces the common parameter vector $\mathbf{P_c}$ for the reflection and transmission experiments to

$$\mathbf{P_c} = \{\tau_2, \tau_3, \tau_4, Z_{1,2}, \alpha_{L2}, \beta_{L2}, Z_{2,3}, \alpha_{L3}, \beta_{L3}\}. \tag{19}$$

Note that although d_2 and d_4 are expected to be equal, the delays τ_2, τ_3, and τ_4 are estimated, since small differences in thickness can have an important influence on the phase characteristic of the reflection and transmission experiments in the considered frequency range.

III. The Estimation of the Model Parameters

The estimation of the model parameters $\mathbf{P_r}$ and $\mathbf{P_t}$ is elaborated using a Maximum Likelihood (ML) approach (reflection or transmission data). In [16], the identification of transfer function models for linear time invariant systems is treated in an ML sense. A similar approach was followed for the identification of parametric models for reflection and transmission experiments performed on a viscoelastic plate [7], [15].

The ML estimator (MLE) for linear systems constructed in [16] requires the measured input $X_j(\omega)$ and output $Y_j(\omega)$ spectra of the system under investigation, as well as knowledge of the perturbing noise variances. Furthermore, the noise sources are assumed to be zero mean complex normal distributed. If the measured spectra of input and output are obtained using a Discrete Fourier Transform, this assumption is valid [17]. Although the reflection or transmission models defined in (9) are nonlinear with respect to the model parameters $\mathbf{P_r}$ and $\mathbf{P_t}$, it can be shown that the basic assumptions necessary to apply the ML approach are still valid in this case. A more elaborate analysis of the developed MLE can be found in [7] and [15].

The nonparametric estimates occurring in (7) and (8) are obtained from averaging the input-output measurements during the calibration experiments and the reflection and transmission experiments, respectively

$$H_j^{np}(\omega) = \exp\left(\frac{1}{M}\sum_{i=1}^{M} \log\left(\frac{Y_j^i(\omega)}{X_j^i(\omega)}\right)\right) \quad \text{with} \quad j = \text{calr, calt}, mr, mt. \tag{20}$$

Since the generation and acquisition of the signals are not perfectly synchronized, the measurements are averaged using the $H_{\log}$ technique [18]. During the averaging procedure, the variances on the nonparametric estimates $\sigma^2_{H_j^{np}}(\omega)$ are determined as well. Due to the high signal-to-noise ratio of the input and output spectra (typically 40 dB), the $H_{\log}$ estimates will still be complex normal distributed, so that the assumptions on the noise properties are also justified. Taking into account these considerations, the cost functions C_r, C_t to be minimized in ML sense are given by [7], [17]

$$C_r(\mathbf{P_r}) = \sum_{l=1}^{F} |e_r(\omega_l, \mathbf{P_r})|^2 \quad \text{and}$$
$$C_t(\mathbf{P_t}) = \sum_{l=1}^{F} |e_t(\omega_l, \mathbf{P_t})|^2 \tag{21}$$

with

$$e_i(\omega_l, \mathbf{P_i}) = \frac{H^{np}_{\text{cali}}(\omega_l) \cdot \tilde{H}_i(\omega_l, \mathbf{P_i}) - H^{np}_{mi}(\omega_l)}{\sqrt{\sigma^2_{H^{np}_{\text{cali}}}(\omega_l) \cdot |\tilde{H}_i(\omega_l, \mathbf{P_i})|^2 + \sigma^2_{H^{np}_{mi}}(\omega_l)}} \quad \text{with} \quad i = r, t \tag{22}$$

and where $\{\omega_l, l = 1, \cdots, F\}$ denotes the set of angular frequencies taken into account. The nonparametric estimates of the inputs and outputs, as well as their variances, are determined at each spectral line l as explained before (see (20)). Finally, $\tilde{H}_i(\omega_l, \mathbf{P_i}) (i = r, t)$ represents the transfer function models as defined in (9) evaluated at the l-th spectral line. Equation (21) gives rise to a nonlinear minimization problem.

The order selection for the rational form modeling the absorption-dispersion behavior of the sample is based on a comparison of the value of the cost functions C_r and C_t obtained from estimations performed with different model orders. The model order is increased as long as an important decrease of the cost functions is observed. Furthermore, in [16], it is shown that when no model errors are present, the theoretical value of the cost function equals

$$C_i = F - \frac{n_{pi}}{2} \quad \text{with} \quad i = r, t \tag{23}$$

with n_{pi} the number of parameters to be estimated for reflection and transmission, respectively. By comparing the value of the cost function obtained during the order selection procedure with the theoretical value (23), conclusions can be drawn concerning the presence of model errors.

The initial parameter values for the thickness of the specimen and density are obtained from basic experiments, while the dispersionless phase velocity comes from the literature [3]. Initial values for the numerator and denominator coefficients of the rational transfer function are not available. However, this problem was solved by starting the estimation only with a first-order model ($N_i = 1, D_i = 0$) or ($N_i = 0, D_i = 1$), and selecting a very small parameter value [7]. After minimizing (21), the model order is gradually increased and the previously obtained estimation results are used as initial parameter values, while the newly added coefficient, again, is chosen to be very small. Since the initial parameter values of the other parameters are determined within a measurement accuracy of 10%, the minimization does not suffer from the presence of local minima.

In the next section, the constructed MLE is applied to the experiments performed on the sediments.

IV. The Experimental Results and Discussion

Experiments and discussions following hereafter present detailed results for the Boom Clay sample. The results of the sand sample are not widely discussed because no satisfactory results could be obtained, partly due to limitations of the current measurement setup. A validation experiment in the case where the plexi container is filled with water is included. It illustrates the accuracy of the used plane wave model for an ideal medium (dispersionless and absorptionless, isotropic, homogeneous, and linear in the used frequency band of 300 to 700 kHz).

For the example proposed for discussion here, the parameters that characterize the walls of the Plexiglas container are kept fixed along the estimations of the parameters for the sediment sample. Other calculations where the delays at the walls had been estimated along with the sediment parameters did not contribute to a better model for the sediments.

The parameter vector of one wall of Plexiglas $\mathbf{P_{L2}}$ is assumed to characterize the two walls of the Plexiglas container, that is, $\mathbf{P_{L2}} = \mathbf{P_{L4}} = \mathbf{P}_{pl}$. $\mathbf{P_{L2}}$ is obtained from previous estimations for a Plexiglas plate and for the container filled with water, both measured in transmission. The results of these estimations for the Boom Clay are presented in Table I, together with the ones for $\mathbf{P_{L2}}$ that are marked "fixed" and that serve as input data for the estimations, both in transmission and reflection. The parameters and their uncertainties correspond to a model ($N_i = 2, D_i = 1$) for layers $i = 2, 3$. The model order (2, 1) was then selected after following the model order selection as explained in Section III.

It is important to note that errors due to the estimation of the parameter vector $\mathbf{P_{L2}}$ are further introduced into the estimation of the sediment parameters. Nevertheless, these errors influence the results of the estimations for both the transmission and reflection experiments in the same manner. The specific estimations for reflection, nevertheless, hold uncertainties that are systematically higher than the ones for transmission, which indicates that the quality of the estimates deduced for the former is less reliable than that for the latter. The ratios $Z_{2,3}$ obtained from reflection and transmission data have comparable magnitude, but further estimates of $\alpha_{3,1}, \alpha_{3,2}, \beta_{3,1}$ differ significantly. Based on the better quality of the transmission estimates then, these results for an ($N_3 = 2, D_3 = 1$) order of the absorption-dispersion model are discussed next.

TABLE I
The Estimated Model Parameters and Their Uncertainty for Reflection and Transmission Data for the Boom Clay Sample

	P_r	P_t	comment
τ_R (s)	-1.9425e-7 (0.0005e-7)	—	
τ_T (s)	—	2.68400e-5 (0.00007e-5)	
$\tau_2\,(s)$	3.776e-6 (0.001e-6)	3.776e-6 (0.001e-6)	fixed
$Z_{1,2}$	2.0554 (0.0006)	2.0554 (0.0006)	fixed
$\alpha_{2,1}$	7.57e-7 (0.06e-7)	7.57e-7 (0.06e-7)	fixed
$\alpha_{2,2}$	7.8e-16 (0.2e-16)	7.8e-16 (0.2e-16)	fixed
$\beta_{2,1}$	7.25e-7 (0.06e-7)	7.25e-7 (0.06e-7)	fixed
τ_3 (s)	1.412e-5 (0.005e-5)	1.3578e-5 (0.0001e-5)	
$Z_{2,3}$	0.620 (0.002)	0.6321 (0.0005)	
$\alpha_{3,1}$	3.7e-6 (0.3e-6)	5.67e-7 (0.08e-7)	
$\alpha_{3,2}$	1.5e-14 (0.1e-14)	2.20e-15 (0.04e-15)	
$\beta_{3,1}$	3.4e-6 (0.2e-6)	5.55e-7 (0.08e-7)	

Fig. 5 shows the magnitude and phase characteristics of the measured and estimated transmission coefficients, and of the magnitude and phase differences for water in place of the sediment in the plexi container. The results for the Boom Clay sample are given in Fig. 6. Comparing the magnitude and phase differences in Fig. 5(c) and (d) with Fig. 6(c) and (d), it is concluded that the accuracy of both estimates is comparable. Magnitude differences of 0.3 dB are observed and the phase differences are within three degrees. Moreover, the experimental value of the cost function for the Boom Clay sample, $C_t = 7544$ (expected value $C_t = 64$), is quite similar to $C_t = 6271$ obtained for water. This confirms the validity of the proposed absorption-dispersion model for a multilayer, and also that the Boom Clay can be regarded as a linear, homogeneous, isotropic visco-elastic medium in the frequency range used. However, it indicates that other loss mechanism should be considered when a better accuracy is envisaged. In addition, the absorption and dispersion characteristics of the Boom Clay sample are depicted in Fig. 7(a) and (b), where it is apparent that dispersion effects are small in the frequency range of our experiments.

The ($N_2 = 2, D_2 = 1$) estimation for one layer of Plexiglas of 0.02 m (water/Plexiglas/water system where $n = 2$) results in a cost function of $C_t = 1204$, which indicates that errors due to diffraction at a complex multilayer ($n = 4$) are readily present. Moreover, shear waves have not been considered. Nevertheless, it should be noted that the experimental cost function itself (21) is weighed with respect to the variances of

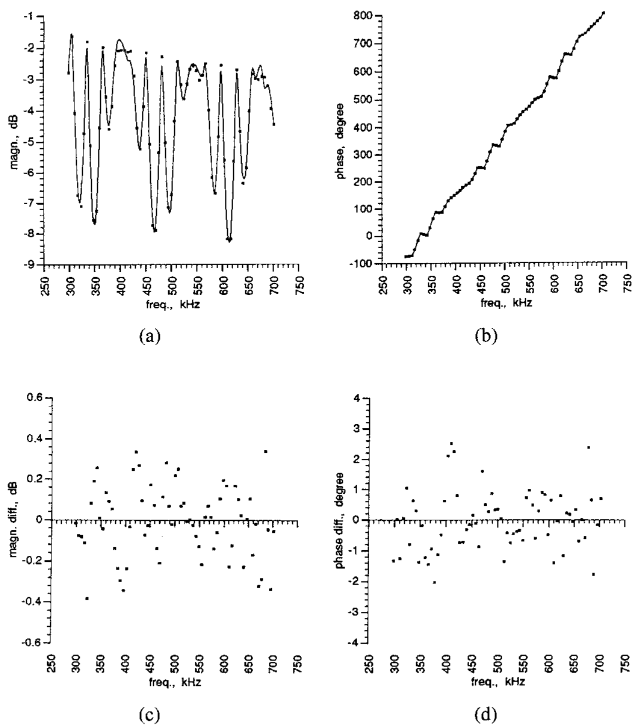

Fig. 5. The estimation results in transmission for the plexi container filled with water. (a) The magnitude of the measured (■) and estimated (–) transfer function. (b) The phase of the measured (■) and estimated (–) transfer function. (c) The magnitude difference between the estimated and measured transfer function (■). (d) The phase difference between the estimated and measured transfer function (■).

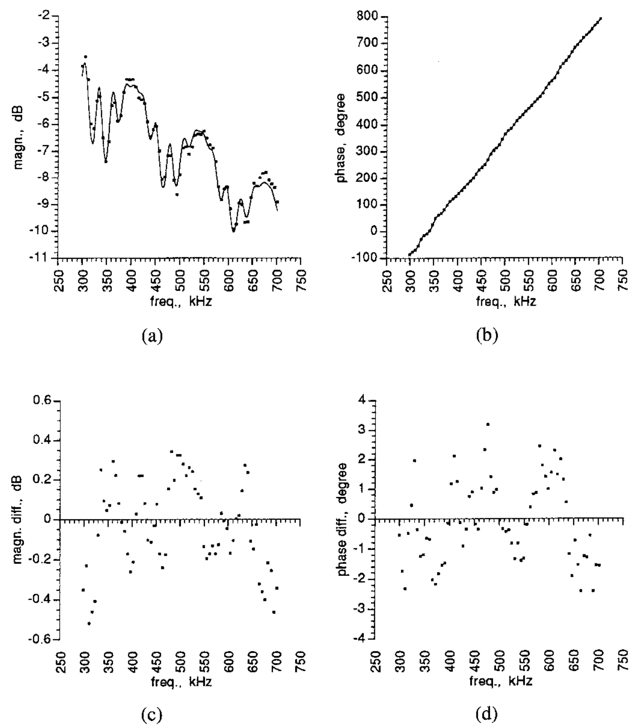

Fig. 6. The estimation results in transmission for the Boom Clay. (a) The magnitude of the measured (■) and estimated (–) transfer function. (b) The phase of the measured (■) and estimated (–) transfer function. (c) The magnitude difference between the estimated and measured transfer function (■). (d) The phase difference between the estimated and measured transfer function (■).

the measurements, which are also experimentally determined, and therefore can enlarge the cost function value.

In order to illustrate our approach applied to a sediment with different geo-mechanical characteristics, the sand sample presented in Section I was examined. However, due to its high absorption, the signal to noise ratio was too low for the experiments held in transmission, thus only reflection data could be used, which readily brings forward errors due to the calibration procedure followed. Indeed, the estimation results in a cost function $C_r = 28451$ for a $(N_3 = 1, D_3 = 1)$ rational form, as compared to $C_r = 16636$ for a $(N_3 = 1, D_3 = 1)$ model for mud measured in reflection. Selecting higher model orders did not improve the estimations because uncertainties on the parameters became too high. Despite the calibration constraints (and the diffraction effects), the latter comparison confirms the necessity of using a more elaborate model which describes other mechanisms of energy losses characteristic of a two-phase (sediment solid frame and saturating brine) media as proposed in [4], [5], [19], and [20].

V. Conclusion

In this paper, a system identification approach for the parametric modeling of ultrasonic wave propagation through marine sediments has been elaborated. Using a validation experiment, it has been demonstrated that a silty-clay sample of the characteristics of the Boom Clay can be modeled by the transfer function developed under the assumption of

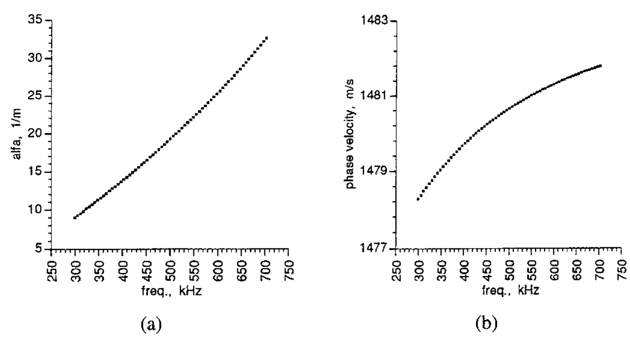

Fig. 7. The estimated absorption (a) and dispersion (b) for the Boom Clay sample (transmission).

visco-elastic response of a one-phase medium, and considering absorption and dispersion.

With the encouraging results obtained from the experiments on the Boom Clay sample, one can propose that the current approach is useful for identifying muds, namely silty clays of low density (<1500 kg $\cdot$ m^{-3}) encountered in marine environments that can be described essentially by a one-phase medium.

The parametric identification of the sand sample was less satisfactory due to the fact that the physical mechanism of acoustic wave propagation in sediments having this granulometric distribution and sorting is more complicated than proposed.

If more precise estimations are needed as for a sediment, the granular and fluid parts of which may respond as a two-phase medium (e.g., sand, sandy silt, and even muds with a poor sorting), the model proposed by Biot [19], [20] and modified by Stoll [4], [5] appears to be a logical alternative to ameliorate the parametric wave propagation modeling. Nevertheless, the general framework of the inverse problem presented here remains valid. It allows the incorporation of more elaborated models describing the underlying physical phenomena of acoustic wave propagation in marine sediments and the incorporation of diffraction corrections.

ACKNOWLEDGMENT

The authors want to thank Prof. S. Wartel (KBIN: Royal Belgian Institute of Natural Sciences), and Prof. R.W. Faas (Lafayette College—Geology Department) for fruitful discussions and support for the sedimentologic experiments.

REFERENCES

[1] E. Hamilton, "Sound velocity and related properties of marine sediments, North Pacific," *J. Acoust. Soc. Amer.*, vol. 75, no. 23, pp. 4423–4446, Aug. 1970.

[2] ——, "Compressional-wave attenuation in marine sediments," *Geophysics*, vol. 37, no. 4, pp. 620–646, Aug. 1972.

[3] ——, "Geoacoustic modeling of the sea floor," *J. Acoust. Soc. Amer.*, vol. 68, no. 5, pp. 1313–1339, Nov. 1980.

[4] R. D. Stoll, "Acoustic waves in saturated sediments," in *Physics of Sound in Marine Sediments.* New York: Plenum, 1974, vol. 1 (Marine Sci.), pp. 19–37.

[5] ——, "Theoretical aspects of sound transmission in sediments," *J. Acoust. Soc. Amer.*, vol. 68, no. 5, pp. 1341–1350, Nov. 1980.

[6] D. J. Wingham, "The dispersion of sound in sediment," *J. Acoust. Soc. Amer.*, vol. 78, no. 5, pp. 1757–1760, Nov. 1985.

[7] L. Peirlinckx, R. Pintelon, and L. Van Biesen, "Identification of parametric models for ultrasonic wave propagation in the presence of absorption and dispersion," *IEEE Trans. Ultrason., Ferroelec., Freq. Contr.*, vol. 40, no. 4, pp. 302–312, July 1993.

[8] L. Bjørnø, "Wave propagation through marine sediments," *Acustica*, vol. 38, no. 4, pp. 196–200, 1977.

[9] S. Heltzel and M. Teeter, "Settling of cohesive sediments," *Coastal Sediments*, pp. 63–70, 1987.

[10] S. Wartel and P. S. Sethi, "Effect of overburden pressure on clay fabric," *Bullet. van het Koninklijk Belgisch Inst. Natuurwetenschappen (KBIN), Aardwetenschappen*, vol. 61, pp. 227–230, 1991.

[11] M. D. Richardson, P. V. Curzi, E. Muzi, F. Turgutcan, and T. Akal, Saclantcen Rep. SR-199, Oct. 1992.

[12] L. Hampton, "Acoustic properties of sediments: An update," *Rev. Geophysics*, vol. 23, no. 1, pp. 49–60, Feb. 1985.

[13] R. W. Faas, "Time and density-dependent properties of fluid mud suspensions, NE Brazilian continental shelf," *Geo-Marine Lett.*, vol. 4, pp. 147–152, 1987.

[14] ——, "Viscous control of estuarine resuspension patterns," *Coastal Sediment*, pp. 300–315, May 1987.

[15] L. Peirlinckx, P. Guillaume, R. Pintelo, and L. Van Biesen, "MIMO identification of parametric models for ultrasonic reflection and transmission experiments," in *Proc. IEEE Ultrason. Symp.*, Baltimore, MD, vol. 2, pp. 723–728, Oct. 31–Nov. 3, 1993.

[16] J. Schoukens and R. Pintelon, *Identification of Linear Systems, A Practical Guideline to Accurate Modeling.* New York: Pergamon, 1991.

[17] J. Schoukens and J. Renneboog, "Modeling the noise influence on the Fourier coefficients after a discrete Fourier transform," *IEEE Trans. Instrum. Meas.*, vol. IM-35, pp. 278–286, Sept. 1986.

[18] P. Guillaume, R. Pintelon, and J. Schoukens, "Nonparametric frequency response function estimators based on nonlinear averaging techniques," *IEEE Trans. Instrum. Meas.*, vol. 41, no. 6, pp. 739–746, Dec. 1993.

[19] M. A. Biot, "Mechanics of deformation and acoustic propagation in porous media," *J. Applied Physics*, vol. 33, pp. 1482–1498, 1962.

[20] ——, "Generalized theory on acoustic propagation in porous dissipative media," *J. Acoust. Soc. Amer.*, vol. 34, pp. 1254–1264, 1962.

Zobeida Cisneros was born in Guayaquil, Ecuador, in 1965. In 1989, she graduated as an Engineer in geology at the Escuela Superior Politecnica del Litoral (ESPOL), Guayaquil. Her research pointed to the prospection of gold and groundwater. From 1990 to 1992, and with support of the Belgian Agency for Cooperation and Development (ABOS), she entered the master's program in Fundamental and Applied Quaternary Geology (IFAQ) at the Vrije Universiteit Brussel (VUB).

In 1992, she joined the Department of Fundamental Electricity and Instrumentation (ELEC) of the Free University of Brussels. In the frame of the modeling of the North Sea, her work points to the relations between the geo-mechanics of marine sediments and the acoustic measurements on them.

Luc Peirlinckx was born in Aalst, Belgium, on June 25, 1965. He graduated as an Electro-Mechanical Engineer in applied physics at the Vrije Universiteit Brussel (VUB), Brussels in 1988. His research activities were situated in the domain of nonlinear optics: optical bistability. In 1989, after joining the Department of Fundamental Electricity and Instrumentation of the Free University of Brussels (VUB), he received a fellowship from the Belgian Institute for the Encouragement of the Research in Industry and Agriculture (IWONL). He received the doctorate degree in applied sciences in June 1994 from the same university (VUB).

In October 1994, he became a part-time Lecturer and teaches a course on fundamental electricity. His main research interests are underwater acoustic wave propagation, parameter estimation, and system identification.

Leo Pierre Van Biesen was born in Elsene, Belgium, on August 31, 1955. He received the degree of Electro-Mechanical Engineer from the Free University of Brussels (Vrije Universiteit Brussel), in 1978, and the doctoral degree (Ph.D. equivalent) from the same university in 1983. From 1978 to 1982, he worked under a fellowship from the Belgian Institute for the Encouragement of the Research in Industry and Agriculture (IWONL). In this period, he carried out research on automated cable fault location techniques, which led to completion of the doctoral degree. This work was done in cooperation with the Belgian company Balteau.

In 1983, he was appointed a Senior Assistant in the Department of Fundamental Electricity and Instrumentation of the Free University of Brussels. He started his career as a Lecturer after 1984, when he was nominated to be a part-time Lecturer. In 1985, he joined the Rectoral Services of the same university to be in charge of the management of the R&D Department of the university. He occupied this function until 1987. In 1988, he became a full-time Lecturer (Professor). He teaches courses on fundamental electricity, electrical measurement techniques, signal theory, computer controlled measurement systems, and telecommunication. In 1994, he became Senior Professor at the Free University of Brussels. He is also the Director of the "Earth Technology Institute" of the Free University of Brussels. His current interests are signal theory, modern spectral estimators, time domain reflectometry, underwater acoustics, and expert systems for intelligent instrumentation. He is also active in the fields of automatic navigation, ECDIS, and marine GIS systems, and has developed, in cooperation with the Belgian company Tresco, an automatic navigation system for ships called PC-NaviGIS.

Dr. Van Biesen was awarded the 100th Anniversary Award of the Royal Belgian Electrotechnique Society for his doctoral research work in 1984. He has been the Belgian delegate in the International Measurement Confederation (IMEKO) since 1993, and Chairman of the IMEKO Technical Committee on Measurement Science.